Temperature-sensitive splicing defects in Arabidopsis mitochondria caused by mutations in the ROOT PRIMORDIUM DEFECTIVE 1 gene

Chuande Wang, Martine Quadrado, Hakim Mireau

Nucleic Acids Research, 2024, 1–13
https://doi.org/10.1093/nar/gkae072
RNA and RNA-protein complexes

Temperature-sensitive splicing defects in Arabidopsis mitochondria caused by mutations in the ROOT PRIMORDIUM DEFECTIVE 1 gene

Chuande Wang[1], Martine Quadrado[2] and Hakim Mireau[2,*]

[1]School of Agriculture and Biology, Joint Center for Single cell Biology/Shanghai Collaborative Innovation Center of Agri-Seeds, Shanghai Jiao Tong University, Shanghai, China
[2]Université Paris-Saclay, INRAE, AgroParisTech, Institut Jean-Pierre Bourgin (IJPB), 78000 Versailles, France
[*]To whom correspondence should be addressed. Tel: +33 130 833 070; Fax: +33 130 833 319; Email: hakim.mireau@inrae.fr

Abstract

Group II introns in plant organelles have lost splicing autonomy and require the assistance of nuclear-encoded trans-factors whose roles remain to be elucidated. These factors can be mono- or poly-specific with respect to the number of introns whose splicing they facilitate. Poly-acting splicing factors are often essential and their genetic identification may benefit from the use of conditional mutations. Temperature-sensitive (TS) mutations in the *ROOT PRIMORDIUM DEFECTIVE 1* (*RPD1*) gene were initially selected for their inhibitory effect on root formation in Arabidopsis. Further analysis revealed that *RPD1* encodes a mitochondria-targeted RNA-binding protein family member, suggesting a role in mitochondrial gene expression and making its role in root formation enigmatic. We analysed the function of RPD1 and found that it is required for the removal of 9 mitochondrial group II introns and that the identified TS mutations affect the splicing function of RPD1. These results support that the inhibition of adventitious root formation at non-permissive temperature results from a reduction in RPD1 activity and thus mitochondrial activity. We further show that RPD1 physically associates *in vivo* with the introns whose splicing it facilitates. Preliminary mapping indicates that RPD1 may not bind to the same regions within all of its intron targets, suggesting potential variability in its influence on splicing activation.

Graphical abstract

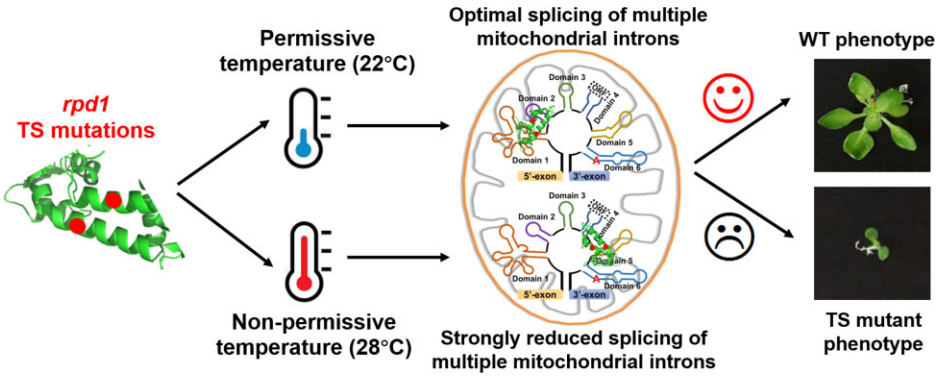

Introduction

Most of our comprehension of biological processes and their underlying mechanisms has been acquired through methods that interfere with regular gene activity, primarily by utilizing loss-of-function mutations. In the case of essential genes whose functionality cannot be completely lost, conditional mutations have proven to be a useful way of avoiding the lethality associated with knock-out mutations in such genes. These include temperature-sensitive (TS) mutations, which have the advantage of inactivating genes without altering their transcriptional context. By simply changing the temperature at which mutants are grown, TS mutant proteins can be studied in a context where they either retain normal function at a permissive temperature or partially lose function at a non-permissive temperature. In budding yeast, the search for TS alleles has been extremely useful in elucidating many molecular pathways (1,2).

In plants, the number of equivalent studies is much more limited, and TS mutations have often been sought to better understand the molecular processes or signalling pathways underlying plant morphology and development (3–6). Among these, TS mutations affecting plant root growth have been identified, most likely because root growth is an easy trait to monitor *in vitro*, at different temperatures (7,8). TS

Received: August 8, 2023. **Revised:** January 6, 2024. **Editorial Decision:** January 20, 2024. **Accepted:** January 25, 2024

mutations in one of such genes called *ROOT PRIMORDIUM DEFECTIVE 1* (*RPD1*) were selected after screening of mutagenized populations of *Arabidopsis thaliana* for their incapacity to form adventitious roots from hypocotyl explants *in vitro* at elevated temperature (8). *rpd1-1* and *rpd1-2* mutants develop normal lateral roots when grown at 22°C, whereas at 28°C root primordia are initiated up to the two-cell layer stage and remain undeveloped with no recognizable apical meristems even after 16 days of incubation on root-inducing medium (9). This led the authors to postulate that the *RPD1* gene may affect the maintenance of meristematic activity and thus the development of adventitious roots without preventing earlier processes involved in primordium differentiation. However, the growth of undifferentiated cell mass (callus) from hypocotyls or root explants was also disrupted at 28°C in *rpd1* mutants, suggesting that *rpd1* TS mutations may affect cell proliferation more broadly and not be limited to the proliferation of root primordium cells.

Positional cloning of the *RPD1* gene revealed that it corresponds to the AT4G33495 gene, which encodes a 409-amino acid protein belonging to a small family of plant-specific proteins consisting of 15 members (9). Next, it was found that this family of proteins shared a new and previously unknown RNA-binding domain, which was later named the Plant Organellar RNA Recognition (PORR) domain (10). PORR proteins have a similar structural organization containing numerous α-helices (Supplementary Figure S1) mediating RNA association (10–12), but it remains unclear how this structure enables RNA binding. Moreover, most PORR proteins are predicted to localize to either chloroplasts or mitochondria (10).

The founding member of the PORR family was the maize WTF1 protein, which, upon association with the RNase III-domain protein RNC1 and other splicing factors, facilitates the splicing of a large number of group II introns in plastids (10). WTF1 was shown to associate with the introns whose splicing it facilitates (10). In Arabidopsis the WTF9 protein was shown to be essential for the splicing of two mitochondrial introns (11). Interestingly, the LEFKOTHEA PORR protein was found to localize to both the nucleus and plastids and assist in the splicing of introns in these two cellular compartments, providing a potential link between the plastid and nuclear intron splicing machineries (12). These recent data have led us to wonder how a PORR protein such as RPD1, which is predicted to be transported into mitochondria, could play a role in root primordia morphogenesis. To better understand the relationship between *RPD1* and root development, we set out to characterize the function of *RPD1* in Arabidopsis mitochondria and determine whether the *rpd1-1* and *rpd1-2* TS mutations uncouple the role of *RPD1* in root morphogenesis from a potential function in mitochondrial gene expression.

Materials and methods

Primers

Oligonucleotides used in this study are listed in Supplementary Table S1.

Plant material

Arabidopsis (*Arabidopsis thaliana*) Columbia-0 (Col-0) and *Landsberg erecta* (Ler) plants were obtained from the Arabidopsis stock centre of the Institut National de Recherche pour l'Agriculture, l'Alimentation et l'Environnement in Versailles (http://dbsgap.versailles.inra.fr/portail/). The T-DNA insertion line SALK_123424 (*rpd1-3*) in the Col-0 genetic background was acquired from the European Arabidopsis Stock Centre (http://arabidopsis.info/). The *rpd1-3* mutants were genotyped by PCR using the primers listed in Supplementary Table S1 and the insertion site was verified by sequencing. The T-DNA insertion in *RPD1* was found to be embryonic lethal, resulting in the absence of homozygous mutant plants in the self-fertilized *rpd1-3* heterozygous plant progeny, as previously reported (9). Seeds for the *rpd1-1* and *rpd1-2* thermosensitive lines (8,9) were kindly provided by Dr Oren Ostersetzer-Biran (The Hebrew University of Jerusalem).

Functional complementation of *rpd1-3* mutants

The full-length coding sequence of *RPD1* was PCR amplified and cloned into the pABI3-GWB13 vector by Gateway™ cloning (Invitrogen). The pABI3-GWB13 vector had previously been constructed to include a 2.5 kb fragment of the *ABI3* gene (AT3G24650) promoter (13). The resulting construct were then transformed into *Agrobacterium tumefaciens* strain C58C51 and introduced into heterozygous *rpd1-3* plants by the floral dip (14). The functionally complemented homozygous mutant plants were identified in the progenies of transformed plants using PCR analysis.

Subcellular localization assay

The RPD1::GFP translational fusion construct was introduced into the PSB-D Arabidopsis cell suspension culture as previously indicated in (15). Prior to imaging, transgenic cells were stained with 0.1 μM Mitotracker™ Red (Invitrogen) to label mitochondria. Fluorescence signals were observed using a Leica TCS SP5 confocal microscope with a 40×/1.25 numerical aperture oil objective. GFP was excited at 488 nm and emitted fluorescence was collected between 500 and 530 nm. Mitotracker™ Red was excited at 561 nm and emitted fluorescence was collected between 580 and 625 nm.

RNA extraction and reverse-transcription quantitative PCR (RT-qPCR)

Total RNA was extracted from 8-week-old flower buds or 14-day-old *in vitro*-grown plantlets using TRIzol reagent (Life Technologies) according to the manufacturer's instructions. RNA was then treated with DNase Max (QIAGEN). First-strand cDNA synthesis was performed with M-MLV Reverse Transcriptase 1st-Strand cDNA Synthesis Kit (Invitrogen). Quantification of mitochondrial transcript and splicing efficiency were performed by quantitative RT-PCR as previously described (16,17). Two biological and three technical repeats were performed and the nuclear 18S ribosomal RNA gene was used for data normalization.

Blue Native gel electrophoresis and in-gel activity assays

Crude membrane extracts enriched in mitochondria were prepared using either eight-week-old flower buds or 14-day-old seedlings, as previously described in (18). An equivalent to 100 μg of total proteins was loaded and separated on 4–16% (w/v) polyacrylamide NativePAGE™ Bis/Tris gels (Invitrogen). After gel electrophoresis, BN-PAGE gels were stained with Coomassie Blue or in buffers revealing the activities of

mitochondrial respiratory complexes I and IV as previously described (19). When sufficient coloration was obtained, gels were transferred to a fixing solution containing 30% (v/v) methanol and 10% (v/v) acetic acid to stop the reactions.

Protein extraction and immunoblotting

To perform immunoblotting after BN-PAGE migration, the gels were transferred onto 0.45 μm polyvinylidene difluoride (PVDF) membranes using liquid transfer conditions in 50 mM Bis/Tris and 50 mM Tricine at 20 V overnight at 4°C. To estimate mitochondrial protein abundance, total proteins were extracted from the crude membrane in a cold lysis buffer containing 50 mM Tris–HCl (pH 7.5), 100 mM NaCl, 5 mM EDTA, 1% (v/v) NP-40, 0.5% (w/v) sodium deoxycholate, 0.1% (v/v) SDS and 1× complete EDTA-free protease inhibitor (Roche). The protein concentrations were assessed using the Bradford method (Bio-Rad). Approximately 30 μg of total mitochondrial proteins were separated on SDS-PAGE gels and transferred onto PVDF membrane under semi-dry conditions (Bio-Rad). Membranes were incubated with specific primary antibodies (Supplementary Table S2) overnight at 4°C. The hybridization signals were then detected using enhanced chemiluminescence reagents (Western Lightning Plus ECL, Perkin Elmer).

RNA immunoprecipitation assays

RNA immunoprecipitation (RIP) experiments were performed using the μMACS GFP-Tagged Protein Isolation Kit (Miltenyi Biotec) according to the manufacturer's instructions. Briefly, Arabidopsis cells expressing the RPD1-GFP translational fusion were collected from a 3-day-old culture and ground into a fine powder in liquid nitrogen. Samples were homogenized in lysis buffer (μMACS GFP Isolation Kit; Miltenyi Biotec) with the Complete Protease Inhibitor Mixture (Roche). The lysates were clarified by ultracentrifugation at 100 000 *g* for 20 min at 4°C and the supernatant collected. A volume corresponding to 7 mg of proteins was incubated with 50 μl of anti-GFP magnetic beads (Miltenyi Biotec) for 1 h at 4°C with rotation (10 rpm). The mixture was then applied onto an equilibrated micro-column (Miltenyi Biotec) to drain the liquid by a gravity flow. Immobilized beads were washed 4 times with 200 μl of wash buffer 1 and 1 time with 100 μl of wash buffer 2 (Miltenyi Biotec). RNAs were extracted from the beads with the TRI reagent (Life Technologies), precipitated with ethanol, and then used for RT-qPCR analysis. Prior to retrotranscription, immunoprecipitated RNAs were treated with DNase I and purified using the RNA Clean & Concentrator Kits (Zymo Research®, CA, USA). For RIP-RTqPCR with RNase I treatment, the clarified lysates were pretreated with 1 U/μl of RNase I (Ambion) at 25°C for 10 min, followed by the same immuno-precipitation procedure as described above. Primer design details for RT-qPCR analysis are provided in Supplementary Figures S6 and S7. Two independent immunoprecipitations and three cDNA syntheses for each sample were used in these analyses. RIP-RTqPCR experiments on untransformed PSB-D cells were used as a negative control.

Accession numbers

Sequence data from this article can be found in the GenBank/EMBL data libraries under accession numbers RPD1, AT4G33495; WTF1, AT4G01037; WTF9, AT2G39120; LEFKOTHEA, AT5G62990.

Results

RPD1 is an essential gene encoding a protein targeted to plant mitochondria

The *RPD1* gene was identified as part of a genetic screen looking for thermosensitive mutations affecting lateral root formation in Arabidopsis (8). Two TS mutations in *RPD1* were selected that allow normal root growth at 22°C but not at 28°C. At the non-permissive temperature, lateral root primordia stop developing after the two-cell layer stage on root-inducing medium, suggesting that RPD1 may be essential for root meristem maintenance but not for early root primordium differentiation. Further analysis suggested that RPD1 may encode a mitochondria-targeted RNA-binding PORR protein, raising questions about the role of RPD1 and mitochondria in root development (9).

Overall, three mutations were reported to affect the Arabidopsis *RPD1* gene (9). The *rpd1-1* and *rpd1-2* TS mutations consist in the conversion of the arginine at position 152 into a tryptophan and in the transition of the glutamic acid residue at position 308 into a lysine, respectively (Figure 1A). A T-DNA insertion (*rpd1-3*) located at the beginning of *RPD1* (Figure 1A) and causing an embryo-lethal mutation was also previously reported (9). It was found that the development of *rpd1-3* mutant embryos was arrested at stages ranging from the globular to the bent cotyledon (9). To obtain sufficient mutant material and determine whether *RPD1* plays a role in mitochondrial mRNA processing, we attempted to rescue the lethality associated with the *rpd1-3* mutation by complementing *rpd1-3* embryos with a construct expressing the *RPD1* gene under the control of the *ABSCISIC ACID-INSENSITIVE3* (*ABI3*) promoter. The *ABI3* promoter was chosen to direct the expression of *RPD1* during embryogenesis in homozygous *rpd1-3* embryos and to limit RPD1 production during vegetative growth, as previously used for the analysis of several other embryonic lethal mutations in Arabidopsis, *e.g.* (13,20). Two independent partially-complemented lines (*rpd1-3*-pABI3#1 and *rpd1-3*-pABI3#2) were obtained using this strategy and used for further experimental analysis (Figure 1B). Both lines displayed a marked slow growth phenotype and many curly leaves when grown in the greenhouse. However, the *rpd1-3*-pABI3#1 line exhibited a less-affected phenotype compared with the *rpd1-3*-pABI3#2 (Figure 1B). This difference of phenotype correlated with the decrease of *RPD1* expression in both mutants, as *rpd1-3*-pABI3#1 plants were found to accumulate more residual *RPD1* transcript compared to the *rpd1-3*-pABI3#2 mutant (Figure 1C).

pABI3-RPD1 plants under-accumulate mitochondrial respiratory complexes I, III, IV and V

Prediction programs strongly suggested mitochondrial targeting of the RPD1 protein (https://suba.live/suba-app/factsheet.html?id=AT4G33495), which needed to be validated. We thus produced Arabidopsis PSB-D transgenic cells (15) expressing a C-terminal GFP translational fusion comprising the full-length coding sequence of the *RPD1* gene. Transgenic cells were analysed by confocal microscopy and GFP fluorescence was detected as small punctate signals in the cytosol, which co-localized with the MitoTracker™ control (Figure 2). No GFP fluorescence was detected in the nucleus or plastids, indicating that RPD1 is exclusively located in the mitochondria. The strict mitochondrial localization of RPD1 leads us to consider that the altered growth of *rpd1-3*-pABI3 plants

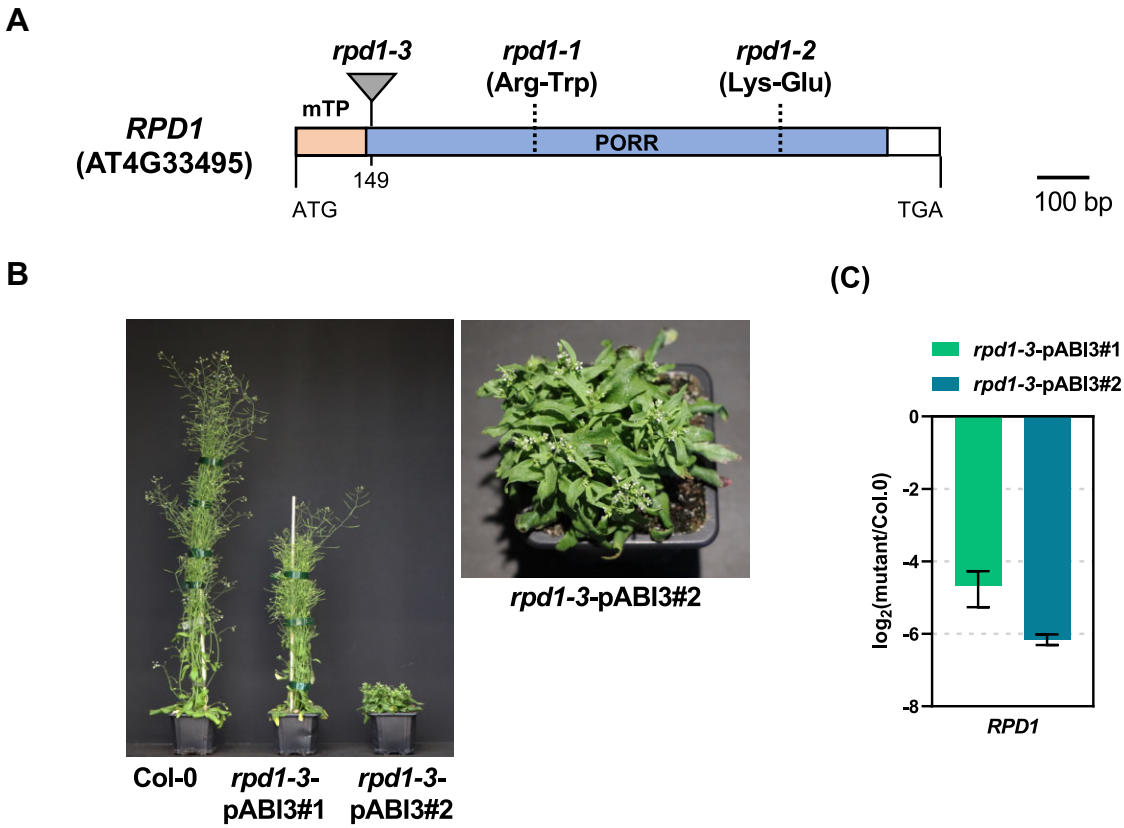

Figure 1. Partially-complemented *rpd1-3*-pABI3 plants display a globally retarded growth phenotype. (**A**) Schematic representation of the *RPD1* gene (AT4G33495) structure, with the putative mitochondrial transit peptides (mTP) and PORR domain highlighted in orange and blue boxes, respectively. The dotted lines indicate the positions of two missense mutations (*rpd1-1* and *rpd1-2*), and the inverted grey triangles indicate the locations of *rpd1-3* T-DNA insertion sites within the gene. (**B**) Photograph of eight-week-old plants showing the global vegetative phenotype of two partially-complemented (*rpd1-3*-pABI3#1 and *rpd1-3*-pABI3#2) plants as compared with the wild type (Col-0). Both partially-complemented plants exhibit strongly reduced size. Magnified view of the *rpd1-3*-pABI3#2 plant, highlighting the twisted and dark green rosette leaves, is shown on the right. (**C**) Quantitative RT-PCR measuring the steady-state levels of *RPD1* mRNA in the two partially-complemented *rpd1-3*-pABI3 plants as compared to the wild-type (Col-0). The histograms show $\log_2$ ratios of *RPD1* mRNA abundance in the mutants to that in wild-type plants.

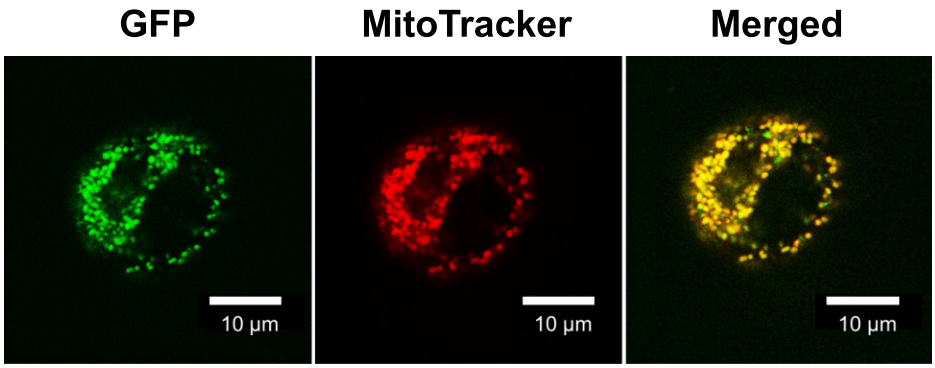

Figure 2. The RPD1 protein is transported into mitochondria. Confocal microscope images showing the subcellular distribution of an RPD1-GFP translational fusion in transgenic Arabidopsis PSB-D cells. The left panel shows the GFP fluorescence, the center panel the mitochondria labelled with the MitoTracker™ Red dye, and the right panel presents the merged signals. The scale bar represents 10 µm.

could be due to changes in the production of the respiratory chain. We therefore examined the integrity of the respiratory chain by monitoring the steady-state levels of the different respiratory complexes in both *rpd1-3*-pABI3 and wild-type plants by blue native polyacrylamide gel electrophoresis (BN-PAGE). Crude mitochondria were purified from both *rpd1-3*-pABI3 and wild-type plants and respiratory complexes solubilized in 1% *n*-dodecyl β-D-maltoside. After separation in BN-PAGE gels, the abundance of respiratory complexes was assessed either by in-gel activity staining or by immunoblotting using antibodies that detect specific respiratory chain subunits. Both in-gel activity staining and immunoblot assay revealed a marked decrease in complex I steady-state level in the two *rpd1-3*-pABI3 lines (Figure 3A). Interestingly, the reduction in complex I was much more pronounced in *rpd1-3-pABI3#2*, with complex I becoming virtually undetectable

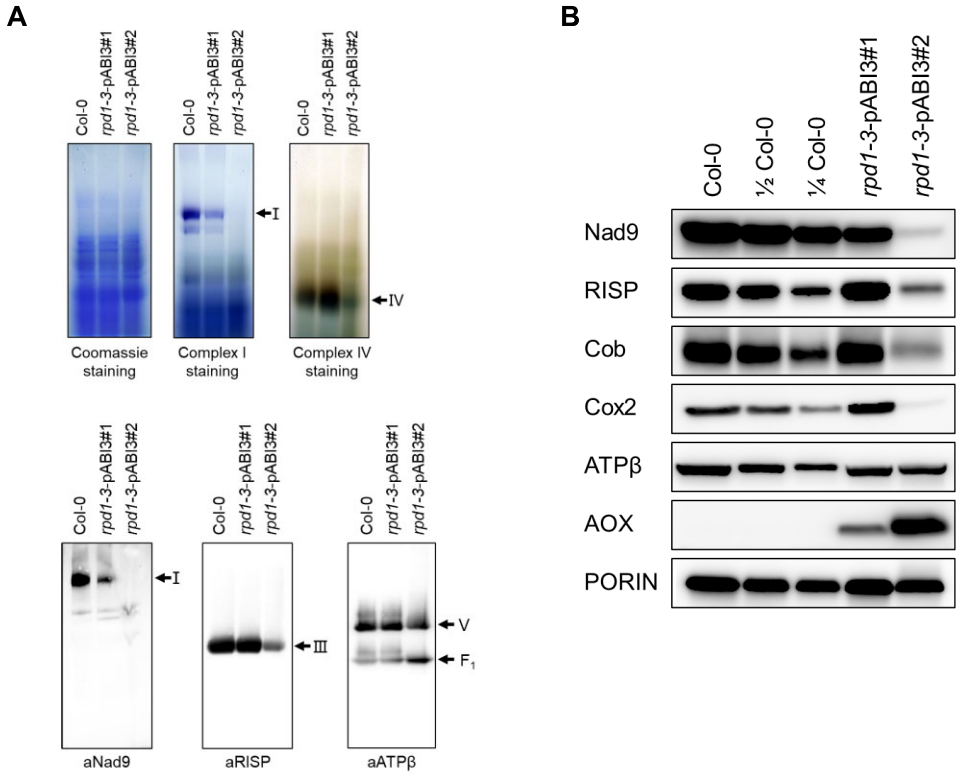

Figure 3. The respiratory chain is altered in partially-complemented *rpd1-3* mutants. (**A**) Crude mitochondrial extracts were prepared from wild-type plants and two partially-complemented *rpd1-3* mutants, and separated on BN-PAGE gels. The gels were then stained with Coomassie blue and subjected to in-gel staining to reveal the NADH dehydrogenase activity of complex I and the cytochrome *c* oxidase activity of complex IV. Following migration, the BN-PAGE gels were transferred to membranes and blots were hybridized with antibodies to mitochondrial Nad9, RISP, and ATPβ. The different respiratory complexes were designated by their roman numeral. (**B**) Assessment of steady-state levels of various mitochondrial proteins in partially-complemented *rpd1-3* mutants. Protein was extracted from the crude membranes of the indicated genotypes and separated by SDS-PAGE. The separated proteins were then probed with antibodies to subunits of complex I (Nad9), complex III (Cob and RISP), complex IV (Cox2), the ATP synthase (ATPβ), and the alternative oxidase (AOX). Porin was used as a protein loading control. Dilution series of proteins extracted from the wild type (Col-0) were used for signal comparison.

in these plants. The analysis of the other complexes also revealed some differences between the two *rpd1-3*-pABI3 lines. While complexes III, IV and V were clearly under-accumulated in *rpd1-3*-pABI3#2, no reduction in these complexes was observed in the less affected *rpd1-3*-pABI3#1 line. On the contrary, a slight over-accumulation of complex IV was detected in the *rpd1-3*-pABI3#1 genotype (Figure 3A). These results were then confirmed by measuring the steady-state levels of several mitochondrial proteins by immunoblot analysis. The obtained results showed significant reductions in Nad9 (a complex I subunit), RISP and Cob (complex III subunits), Cox2 (a complex IV subunit) and Atpβ (a complex V subunit) in the strongly-affected *rpd1-3*-pABI3#2 plants (Figure 3B). Only a slight reduction in Nad9 could be detected in the less-affected *rpd1-3-pABI3*#1 plant. All other tested subunits either over-accumulated (RISP, Cob, Cox2) or were found at wild-type levels (Atpβ) in this genotype. The alternative oxidase (AOX), the terminal component of the alternative pathway that is induced when the respiratory chain is defective, was found to over-accumulate in both *rpd1-3*-pABI3 lines, but much more in *rpd1-3*-pABI3#2 compared to the other line (Figure 3B). In addition, the steady-state levels of the mRNAs encoding the alternative mitochondrial NAD/NADH dehydrogenases (*NDA*, *NDB* and *NDC*) and oxidases (*AOX*) were measured in the partially complemented mutants as well as in wild-type plants using quantitative RT-PCR. The results show that several components of the alternative respiratory pathways, namely the *AOX1A*, *AOX1D*, *NDA1*, *NDB3* and *NDB4* genes, were overexpressed in the mutants by a factor of 4–8 in comparison with the wild type (Supplementary Figure S2). Taken together, these results suggest that the biogenesis and activity of the mitochondrial respiratory chain are disturbed in the *rpd1-3*-pABI3 lines, with a deficiency that appears limited to the complex I in the *rpd1-3*-pABI3#1 plant but that affects the respiratory chain more globally in the *rpd1-3*-pABI3#2 genotype. These analyses therefore reveal a much more degraded respiratory chain in *rpd1-3*-pABI3#2 plants compared to *rpd1-3*-pABI3#1, which correlates perfectly with the difference in phenotype observed between the two lines.

The RPD1 protein is essential for the splicing of nine mitochondrial group II introns

Since previous studies have reported a role for PORR proteins in intron splicing (10–12), we next wondered whether the respiratory chain damage detected in *rpd1-3*-pABI3 plants might be due to defects in mitochondrial mRNA production in these plants. To test this possibility, the steady-state levels of both mature and precursor mitochondrial transcripts were measured by quantitative RT-PCR in both *rpd1-3*-pABI3 and wild-type plants. This approach led us to observe that certain

regions of *nad2*, *nad4*, *nad5* and *nad7* mRNAs as well as the *rps3* transcript under-accumulated in the two partially rescued lines compared to the wild type (Supplementary Figure S3). Again, these reductions were found to be more pronounced in the *rpd1-3-pABI3*#2 plant compared to the other partially-complemented mutant line (Supplementary Figure S3). Since the observed decreases in transcript abundance were localized to mRNA regions surrounding introns, the splicing efficiency of all mitochondrial introns in the mutant plants was measured in comparison to that in the wild type. This led us to detect a reduction in splicing efficiency ranging from 8 to 256 times compared to the wild type for the introns present in these mRNA regions, namely the *rps3* intron, *nad2* intron 2, *nad2* intron 4, *nad4* intron 2, *nad4* intron 3, *nad5* intron 1, *nad5* intron 2, *nad5* intron 3 and *nad7* intron 2 (Figure 4). Of note, the reduction in splicing was 2–4 times greater in *rpd1-3*-pABI3#2 compared to the other line. This analysis thus revealed that RPD1 is indispensable for the splicing of nine mitochondrial group II introns.

The TS mutations in *RPD1* also strongly affect respiratory chain homeostasis and mitochondrial intron splicing

As indicated, two TS mutations affecting adventitious root development were previously selected in *RPD1* (8,9). To better understand whether or not this role of RPD1 in root production is somehow linked to its function in mitochondrial biogenesis, we compared the functionality of the respiratory chain and the splicing activity of mitochondrial introns in *rpd1-1* and *rpd1-2* plants grown at permissive (22°C) and restrictive (28°C) temperatures. For this purpose, wild-type (*Landberg erecta* or *Col-0*), *rpd1-1*, *rpd1-2* and *rpd1-3*-pABI3#1 plants were grown *in vitro* at 22°C and 28°C for two weeks before being collected for molecular analysis. This could not be done with the *rpd1-3*-pABI3#2 line, which produced no seeds. In contrast to wild-type and *rpd1-3*-pABI3#1 plants, which grew quite well at both temperatures, *rpd1-1* and *rpd1-2* mutants grew very poorly at the restrictive temperature (28°C), showing that the effect of these mutations is not limited to root development, but that they have a broad impact on plant growth (Figure 5A). To better understand the origin of these growth changes, we first compared the steady-state abundance of *RPD1* mRNA in *rpd1-1* plants at 22°C and 28°C relative to that in the wild type. There was no significant reduction in *RPD1* transcript abundance at either temperature, suggesting that the TS mutations affect the activity of the RPD1 protein and not on the stability of its transcript (Supplementary Figure S4). The steady-state levels of mitochondrial respiratory complexes were then assessed in plants grown at both temperatures by in-gel activity staining or immuno-detection after BN-PAGE. At permissive temperature, only a slight over-accumulation in complex IV could be detected in *rpd1-1* plants compared to the wild type, whereas, at restrictive temperature, *rpd1-1* plants accumulated strongly-reduced levels of complex I and more of complex IV compared to 22°C (Figure 5B). Analysis of steady-state levels of respiratory chain subunits globally confirmed these observations. Effectively, the loss of complex I at 28°C in *rpd1-1* plants was corroborated by that of the Nad9 subunit and the over-abundance of complex IV correlated with increased levels in Cox2 (Figure 5C). The Cob protein was also found to over-accumulate at 28°C in *rpd1-1* plants, although this was not accompanied with a detectable increase in complex III steady-state level by BN-PAGE immunoblot analysis. A strong over-accumulation of the alternative oxidase (AOX) was also detected at 28°C in *rpd1-1*, which is diagnostic of a perturbed respiratory activity in these plants (Figure 5C). Other proteins analyzed (RISP and ATPβ) were not obviously affected by the culture at restrictive temperature.

Next, we measured the splicing efficiency of all mitochondrial introns in the different mutants (*rpd1-1*, *rpd1-2* and *rpd1-3*-pABI3#1) relatively to the wild type, both at 22°C and 28°C. The 9 introns that were found to be affected in the partially-complemented *rpd1-3*-pABI3 lines were also less efficiently spliced in the two TS mutant lines compared to wild-type plants (Figure 6). At 22°C, the decrease in splicing was similar to that observed in the *rpd1-3*-pABI3 lines (Figure 6). However, the growth at 28°C induces a much greater reduction in splicing efficiency for the nine mitochondrial introns in both TS lines. In fact, measured splicing efficiencies were found to be 5–64 times lower at 28°C than at 22°C for the affected introns. In contrast, the change of growth temperature had no real effect on the splicing pattern found in the *rpd1-3*-pABI3#1 line. These observations are in perfect agreement with the expression of the alternative respiratory pathway genes, which show a strong increase at 28°C compared to 22°C in the *rpd1-1* line, but no major change after the temperature shift in the *rpd1-3*-pABI3#1 line (Supplementary Figure S5).

The RPD1 protein specifically associates *in vivo* with the introns whose splicing it facilitates

Since PORR proteins are RNA binding proteins (10–12), we next wondered if RPD1 would associate *in vivo* with the introns that are much less efficiently spliced in the *rpd1* mutants. To test whether the RPD1 associates with its genetic targets or not, RNA immunoprecipitation assays followed by reverse transcription and quantitative PCR (RIP-qPCR) assays were developed using the Arabidopsis PSB-D cell culture expressing the RPD1-GFP protein fusion (Supplementary Figures S6 and S7). The RPD1-GFP fusion was immunoprecipitated with an anti-GFP antibody and co-enriched RNAs were purified from the coimmunoprecipitation pellets and used for RT-qPCR analysis. A non-transgenic PSB-D line was used as negative control. This approach has been successfully used to identify RNA targets and binding sites of uL18-Like and pentatricopeptide repeat proteins (13,21). When applied to the WTF9 PORR protein (11), it also revealed a meaningful and specific association with its identified intron genetic targets (Supplementary Figure S8). The results obtained with RPD1 show that all introns requiring RPD1 for their splicing were specifically enriched with the RPD1-GFP fusion, strongly supporting that RPD1 associates with its genetically-defined intron targets and thus likely plays a direct role in their removal from mRNAs *in vivo* (Figure 7).

Since RPD1 is involved in the splicing of many different introns, we next wondered whether it would bind to an identical region within these intronic sequences. To answer this question, the co-immunoprecipitation experiments were redone by pre-digesting the extract with the ribonuclease I (RNase I) to narrow down the immunoprecipitated RNA fragment to the region physically covered by RPD1, which would act as a protective factor against the RNase I degradation. The immunoprecipitated RNA fragments were then analyzed by

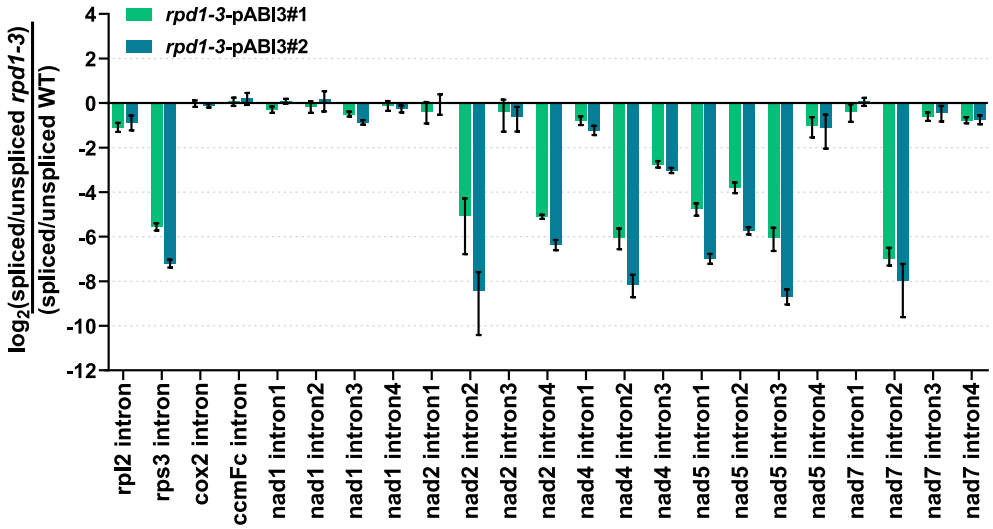

Figure 4. Partially-complemented *rpd1-3* mutants are defective in the splicing of nine mitochondrial introns. Quantitative RT-PCR measuring the splicing efficiency of the 23 mitochondrial introns in Col-0 and partially-complemented *rpd1-3* plants. The histograms show $\log_2$ ratios of mutants to wild type. The PCR amplifications were performed with the primers located in intron-exon junctions and on both sides of introns. Two biological replicates and three technical replicates were used per genotype; standard errors are indicated. The data were normalized to the nuclear 18S rRNA gene.

RT-qPCR using a series of primer pairs scanning whole intron sequences to map the RPD1 binding sites within all the introns to which it associates *in vivo* (Supplementary Figure S6 and S7). We first looked for RPD1 binding sites within the *trans*-introns it targets, namely *nad2* intron 2, *nad5* intron 3 and *nad5* intron 2. In fact, *trans*-introns are formed by the association of two physically separate transcripts, and we wondered whether RPD1 would associate with the same *trans*-intron halves or not. The mapping results clearly showed that this is not the case, as RPD1 associates with the 3′ half of *nad2* intron 2 and the 5′ half of *nad5* intron 3 (Figure 8A and B). The results for *nad5* intron 2 were less clear, as most RNA segments along the intron were co-enriched for RPD1, although a slightly higher enrichment could be detected for segment 1 in the 3′ half of the *trans*-intron (Figure 8C). For the *cis*-introns that require RPD1 for splicing, the results also showed binding to different regions. For *nad2* intron 4, *nad5* intron 1 and *nad7* intron 2, we obtained a clear and strong enrichments in single intron segments (Figure 8D, E and F). For the other 3 *cis*-introns (*nad4* intron 2, *nad4* intron 3 and the *rps3* intron), the mapping results showed enrichments scattered along the introns with one or sometimes two more enriched regions (Figure 8G–I). Overall, this analysis suggests that RPD1 may bind to different regions within its different intron targets, suggesting a sequence-specific mode of RNA recognition rather than a domain-specific association. Therefore, we next aligned the intron segments showing the highest enrichment in RPD1 immunoprecipitation to find potential sequence similarities between them. Unfortunately, no obvious sequence homologies could be detected between these different intron regions (Supplementary Figure S9).

Discussion

RPD1 is a multiple mitochondrial intron splicing factor

The search for conditional mutants in forward genetic screens has long been instrumental in the study of many essential biological processes. This is precisely how the *RPD1* gene was originally identified, in a search for factors governing root development in Arabidopsis (8). Two TS mutations in *RPD1* were selected, which produced plants that were able to form adventitious roots *in vitro* at 22°C, but not at 28°C (8,9). Map-based cloning of the *rpd1* TS mutations revealed that they affected a gene belonging to a then uncharacterised 15-member family, leaving the role of *RPD1* in root growth unexplained at that time. Further analyses later revealed that members of this gene family are indeed RNA-binding proteins involved in organellar intron splicing (10–12). A potential action of *RPD1* in organellar RNA processing was therefore conceivable, while its role in root development remained elusive. To better understand the basis for these two seemingly unrelated functions of *RPD1*, we first determined where the RPD1 protein resides in the cell. Our results confirmed the suspected mitochondrial targeting of RPD1, but not its previously-proposed nuclear localisation (9) (Figure 2). Next, by producing and analysing partially-complemented *rpd1* plants, we revealed that RPD1 is required for the correct splicing of nine mitochondrial introns (6 *cis*- and 3 *trans*-introns), including the one contained in the ribosomal protein gene *rps3* (Figure 4). We then provided further support for the action of *RPD1* in splicing by demonstrating an association of the protein *in vivo* with each of the introns whose splicing is facilitated by RPD1 (Figure 7). This broad action of RPD1 in mitochondrial splicing explains for the multiple respiratory chain defects that we found in *rpd1* knockdown plants (Figure 3) and also the embryonic lethality of *rpd1* knockout mutants (9), but left unexplained the apparent role of *RPD1* in root development. We therefore considered that the two TS mutations that originally linked *RPD1* with root growth might have uncoupled this function of RPD1 from its role in intron splicing. The analysis of the TS mutant phenotype at restrictive temperature (28°C) revealed a global impact on plant development that was not limited to root growth (Figure 5), strongly suggesting a broader impact of the TS mutations on plant cell proliferation. We therefore analysed the organisation of the respiratory chain and measured the splicing ef-

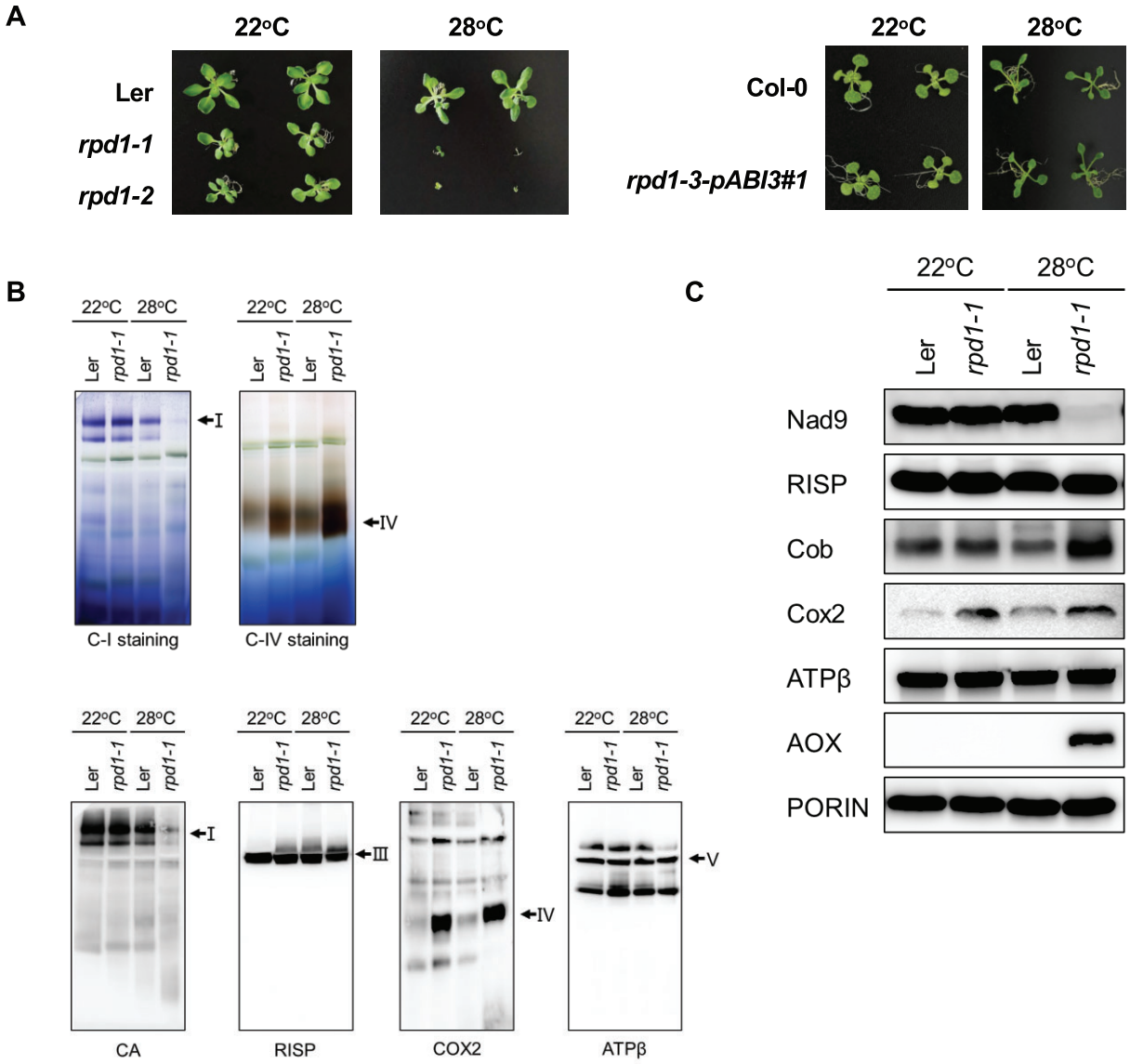

Figure 5. Effects of the temperature-sensitive *rpd1-1* mutation on respiratory complex accumulation. (**A**) Photographs depict the temperature-dependent phenotypes of 14-day-old *rpd1-1* and *rpd1-2* mutants grown *in vitro* at 22°C or 28°C, along with the phenotype of *rpd1-3*-pABI3#1 plants grown under the same conditions. (**B**) BN-PAGE gel analysis of mitochondrial respiratory complex accumulation in *rpd1-1* and wild-type (Ler) plants grown at 22°C or 28°C. The top gels show complex I and IV abundances by activity staining, and the bottom gels show complexes I to V by immunoblot analysis using antibodies to the indicated protein subunits. (**C**) Immunoblot analysis showing the steady-state levels of the indicated mitochondrial proteins in *rpd1-1* and wild-type plants grown *in vitro* at either 22°C or 28°C.

ficiency of mitochondrial introns in the two TS mutants, at both permissive and restrictive temperatures. These molecular analyses revealed that the TS mutants indeed suffer from the same mitochondrial deficiencies as the two *rpd1-3*-pABI3 lines, and that growth at 28°C greatly exacerbates the molecular defects found, notably the impact on the splicing of the nine mitochondrial introns whose splicing depends on RPD1 (Figure 6). These results do not suggest that TS mutations act in root formation independently of the role that *RPD1* plays in mitochondrial RNA processing. Instead, they argue that *RPD1* TS mutations severely reduce mitochondrial activity at 28°C, which in turn inhibits the capacity of cells, including those contained in root primordia, to divide. Since growing the plants under restrictive conditions had no major effect on *RPD1* mRNA abundance (Supplementary Figure S4), the loss of RPD1 activity rather suggests that the protein adopts an inactive structure at 28°C, possibly compromising its RNA binding capacity. Indeed, RPD1 is not the sole case of its kind as three other Arabidopsis TS mutants with altered early-stage adventitious root formation at 28°C were also found to be affected in nuclear genes potentially involved in mitochondrial mRNA processing (22). Other aspects of development like seedling growth or callus formation were also altered by the high temperature treatment in these mutants (8,23), suggesting that the arrest of root growth is most likely caused by mitochondrial misfunctioning and not by a direct role of *RPD1* in root morphogenesis. In effect, mitochondria are not limited to energy production but they also act as signaling organelles to help cells to adapt to various stresses or control cell differentiation during development (24–26). The alteration of mitochondrial activity in plants perturbs cell hormonal and reactive oxygen species (ROS) homeostasis (27,28), whose differ-

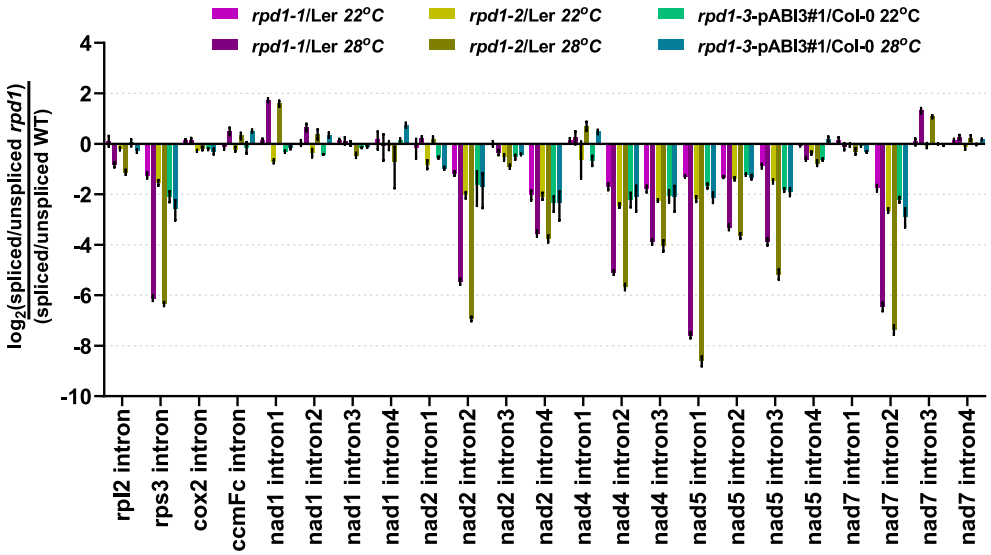

Figure 6. Temperature-dependent effects of the different *rpd1* mutations on mitochondrial intron splicing. Quantitative RT-PCR measuring the splicing efficiency of the 23 mitochondrial introns in *rpd1-1*, *rpd1-2* and *rpd1-3*-pABI3#1 grown at either 22°C or 28°C and relatively to the wild type. The histograms show the $\log_2$ ratios of spliced to unspliced forms for each intron in mutants as compared with the wild type. The data were normalized to the nuclear 18S rRNA gene. Two biological replicates and three technical replicates were used per genotype; standard errors are indicated.

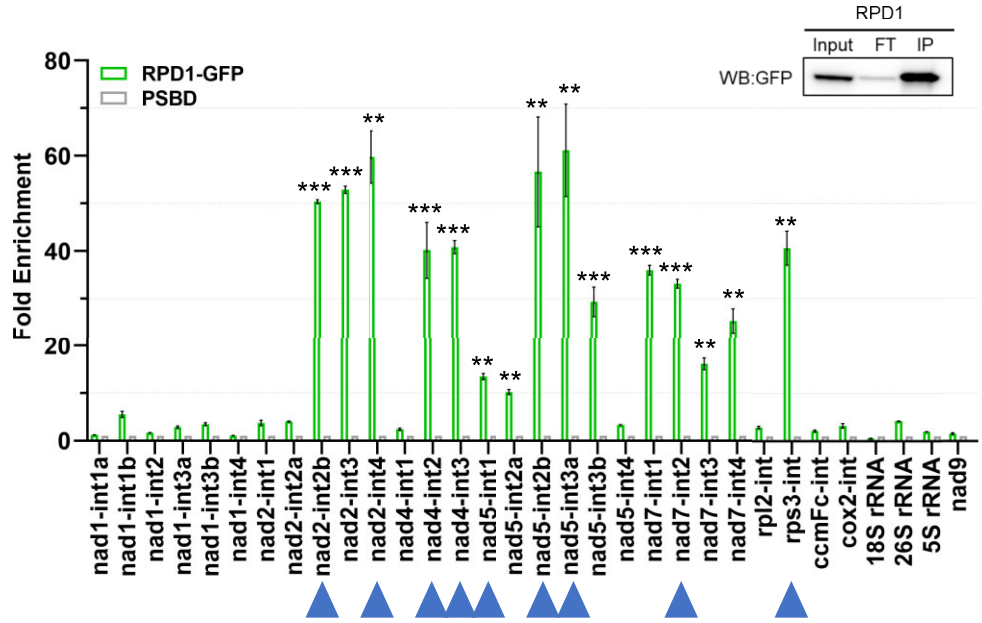

Figure 7. The RPD1 protein associates *in vivo* with its genetically-defined intron RNA targets. In the experiment, total extracts from non-transformed and transgenic RPD1-GFP PSBD cells were subjected to immunoprecipitation using an anti-GFP antibody. Coimmunoprecipitated RNAs were analyzed by qRT-PCR using primer pairs positioned across intron/exon junctions of the indicated mitochondrial transcripts. A graphical overview of the experiment is shown in Supplementary Figure S6. Fold enrichment of the immunoprecipitated (RIP) was calculated as using the $2^{-\Delta\Delta Ct}$ method. Two biological replicates and three technical replicates were used per genotype; standard errors are indicated. *5S*, *18S* and *26S* rRNAs and *nad9* mRNA were used as negative controls, not-targeted by RPD1. Significant differences are indicated with two ($P < 0.01$) or three ($P < 0.001$) asterisks. Blue triangles indicate RPD1 genetic targets. Immunoblot results of total extracts (Input), flow-through (FT) and immunoprecipitated (IP) fractions using the GFP antibody is presented.

ential distribution are known to be essential for the establishment of developmental programs in intact plants and during *de novo* regeneration (29,30). Indeed, changes in mtROS levels act as potent signals to the nucleus to elicit targeted transcriptional responses, known as mitochondrial retrograde signaling, involving a variety of mediators, including transcription factors and cyclin-dependent kinases (31,32). The connection between *RPD1* and root morphogenesis is thus most likely due to the perturbation that its loss induces on mitochondrial activity and on mtROS and hormone homeostasis as a second response. Plant respiratory mutants display a wide range developmental perturbations but how plant meristem differentiation is influenced by mitochondrial homeostasis remains to be determined, yet changes in ROS or hormonal cellular

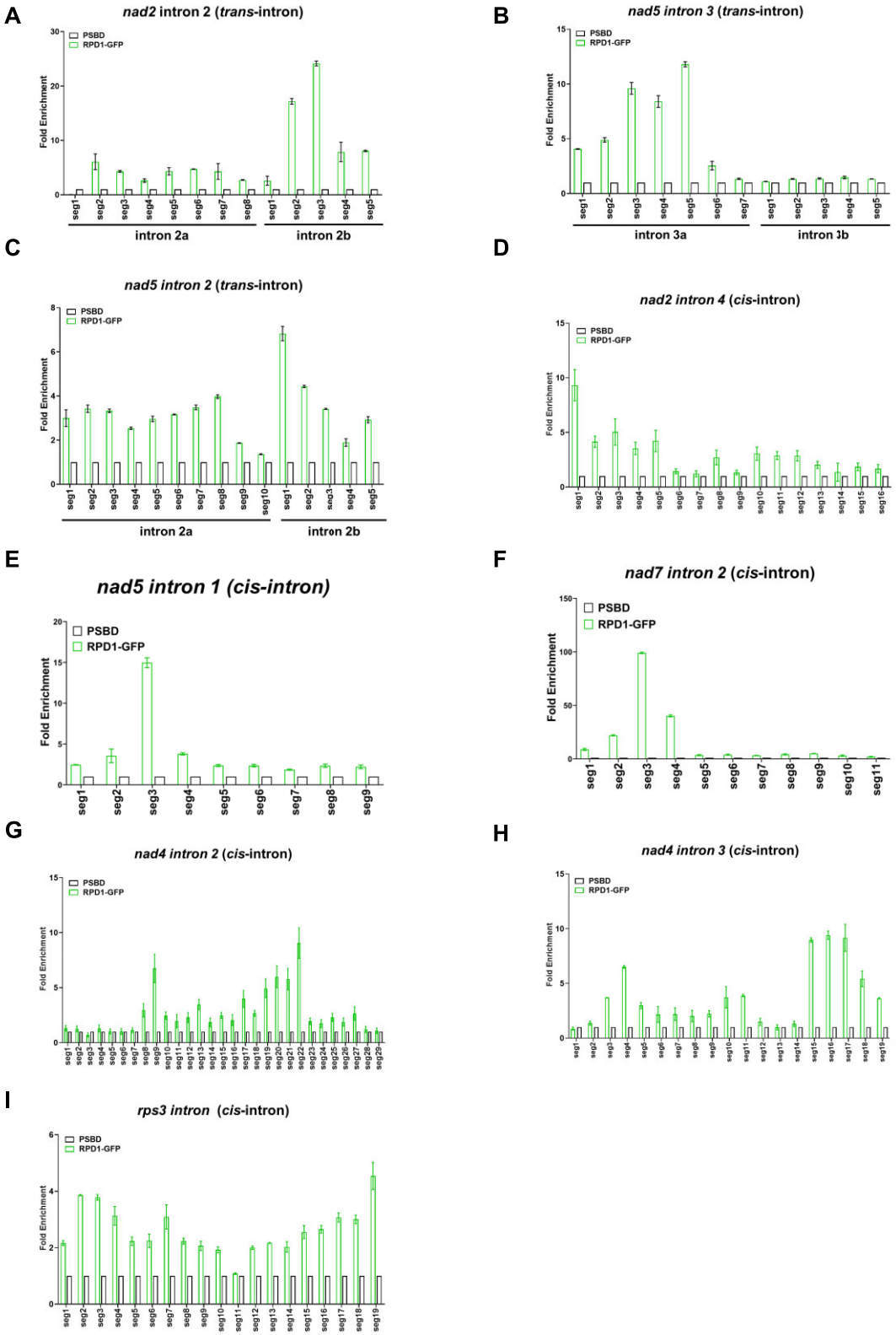

Figure 8. The RPD1 protein does not bind to the same regions within its intron targets. To locate RPD1 binding regions within introns, immunoprecipitated RPD1 protein-intron complexes were digested with RNase I, and protein-protected intron RNA segments were analyzed using RT-qPCR with overlapping amplicons. PCR primer pairs were designed to cover all intron sequences and to generate PCR products overlapping by 150–180 bases. For *trans*-introns, primer pairs were extended to the mapped 3′ and 5′ ends of 3′-half and 5′-half precursors, respectively, as determined in (39) or in Supplementary Figure S7. A graphical overview of the experiment is provided in Supplementary Figure S6. The mapping results for the nine RPD1 intron targets are shown (**A–I**). For the three *trans*-intron targets (*nad2* intron 2, *nad5* intron 3 and *nad5* intron 2), the introns were annotated according to their 5′ and 3′ halves, labelled as 'a' and 'b', respectively. Two biological repeats and three technical repeats were used to produce the shown data.

homeostasis may be at the origin of the observed response. Our data highlight the limitations of phenotype-based genetic screening, where genes with no direct role in development may be identified. Thus, we propose that the primary and most likely sole function of RPD1 is dedicated to the splicing of multiple mitochondrial introns and that its genetic association with root morphogenesis results from by the negative effect that its loss has on mitochondrial functioning and thus on root cell division.

RPD1 may bind to various regions within its intron targets

Introns are intervening DNA sequences that need to be removed from primary RNA transcripts to produce mature mRNAs competent for productive translation. Introns fall into different categories. In plant organelles, they are of bacterial origin and most of them are classified as group II intron RNAs (33). Group II introns are large autocatalytic RNAs, but their splicing and transposition to other DNA sites require the action of an intron-encoded multifunctional protein, which has reverse transcriptase (RT), maturase (splicing) and optionally endonuclease activities (34). The secondary structure of these large introns (which can be larger than 3000 bases in plant mitochondria) consists of six domains (DI-DVI) extending from a central hub and linked by tertiary interactions stabilizing the intron into a catalytically active structure. In addition to their evolutionarily related maturase gene, angiosperm mitochondrial introns have lost many regions essential for splicing. Their splicing thus requires the assistance of many protein cofactors, most of which are nuclear encoded with the exception of the matR maturase encoded in *nad1* intron 4 in angiosperms (35). Several classes of RNA-binding proteins have been shown to assist intron splicing in plant organelles, including proteins of the pentatricopeptide repeat (PPR), mitochondrial transcription termination factor (mTERF), and PORR families, as well as several matR homologs (33). Most of these factors help the splicing of single introns, but some of them, like RPD1, are indispensable for the splicing of many introns, although not always to the same degree. How these proteins assist the splicing is currently unclear, but it has been proposed that they may help introns to fold into a structure competent for splicing (34,36). Some of these *trans*-factors have been shown to interact with other factors involved in splicing but, in most cases, we do not know which intron sequence they associate with. With RPD1, we thought we had an interesting case of a factor required for the splicing of many mitochondrial introns, and we wondered whether or not it binds to the same structural region or sequence within all these introns. Using RNA co-immunoprecipitation analysis, we first observed that RPD1 associates *in vivo* with the 9 introns whose splicing it facilitates. However, for several introns, we did not find a strict correlation between the efficacy of immunoprecipitation and the reduction in splicing measured in *rpd1* mutants. For example, *nad2* intron 2 and 4 were immunoprecipitated with similar efficiency, while *nad2* intron 2 splicing is much more reduced than *nad2* intron 4 splicing in the absence of RPD1 (Figures 4 and 7). In addition, several introns for which we could not detect a decrease in splicing in *rpd1* mutants were efficiently immunoprecipitated with RPD1 (i.e. *nad2* intron 3 or *nad7* intron 1), suggesting that RPD1 may associate with some introns and very weakly facilitate their splicing (Figures 4 and 7). This has also been observed for other multi-intron splicing factors, such as the PORR protein WTF1 (10) or MatR (37), implying that the splicing assistance of this class of *trans*-factors ranges from very minor to highly essential. We then used *in vivo* footprinting analysis (i.e. RIP-RNase I-RTqPCR) to identify the intronic regions to which RPD1 associates *in vivo*. Although this low-resolution approach does not enable precise assessment of co-enriched RNA fragments to specific intronic domains, some general trends have emerged. In *nad2* intron 2 and 4, *nad5* intron 3, *nad5* intron 1, and *nad7* intron 2, the region bound by RPD1 was quite easily identified. The enriched RNA regions were predominantly located in intron 5′ regions. For *nad2* intron 2 and *nad4* intron 3, RPD1 bound to the region located at the opposite end of the intron (Figure 8). Unfortunately, the technology used and the high variability in the sequence and size of group II intron domains makes it difficult to propose more accurate assessments. The mapping results for *nad4* intron 2, *nad5* intron 2 and the *rps3* intron were less clear and scattered over different intronic locations, so no definitive boundaries for the regions bound by RPD1 could be proposed for these introns. These results suggest however that RPD1 may not bind to the same regions within all its intron targets. Rather, RPD1 may recognize similar sequences or RNA structures at different positions in the introns with which it associates. Additional molecular developments are necessary to precisely identify the various RNA sequences bound by RPD1. If RPD1 facilitates the folding of introns into catalytically active structures, our analysis indicates that RPD1 may accomplish this function by targeting different intronic regions. How PORR proteins bind RNA is currently not understood but it has been suggested that they may preferentially associate with single-stranded RNA regions (10). Alignment of the various RNA subregions bound by RPD1 did not reveal any apparent sequence similarities (see Supplementary Figure S9), suggesting a degree of flexibility in the RNA sequences recognized by PORR proteins. Further molecular analyses are therefore required to understand the RNA binding properties of PORR proteins and whether or not their binding really influences the folding of introns into a splicing-competent structures.

During the revision of this manuscript, another analysis of RPD1 has been published (38). Although the genetic material used was different, their conclusions regarding the role of RPD1 in mitochondrial intron splicing were similar to ours. However, the study suggested that RPD1 could bind to both group II intron domains I and V based on the analysis of a single intron, which remains to be verified.

Data availability

The data underlying this article are available in the article and in its online supplementary material.

Supplementary data

Supplementary Data are available at NAR Online.

Funding

Agence Nationale de la Recherche (ANR) [ANR-20-CE11-0021]; The Institut Jean-Pierre Bourgin (IJPB) benefits from the support of Saclay Plant Sciences Grant [ANR-17-EUR-0007]; This work has benefited from the support of IJPB's Plant Observatory technological platforms. Funding for open

access charge: Agence Nationale de la Recherche (ANR) [ANR-20-CE11-0021].

Conflict of interest statement

None declared.

References

1. Li,Z., Vizeacoumar,F.J., Bahr,S., Li,J., Warringer,J., Vizeacoumar,F.S., Min,R., VanderSluis,B., Bellay,J. and DeVit,M. (2011) Systematic exploration of essential yeast gene function with temperature-sensitive mutants. *Nat. Biotechnol.*, **29**, 361–367.
2. Ben-Aroya,S., Coombes,C., Kwok,T., O'Donnell,K.A., Boeke,J.D. and Hieter,P. (2008) Toward a comprehensive temperature-sensitive mutant repository of the essential genes of *Saccharomyces cerevisiae*. *Mol. Cell.*, **30**, 248–258.
3. Sugiyama,M. (2014) Molecular genetic analysis of organogenesis *in vitro* with temperature-sensitive mutants. *Plant Biotechnol. Rep.*, **8**, 29–35.
4. Tamaki,H., Konishi,M., Daimon,Y., Aida,M., Tasaka,M. and Sugiyama,M. (2009) Identification of novel meristem factors involved in shoot regeneration through the analysis of temperature-sensitive mutants of Arabidopsis. *Plant J.*, **57**, 1027–1039.
5. Pickett,F.B., Champagne,M.M. and Meeks-Wagner,D.R. (1996) Temperature-sensitive mutations that arrest Arabidopsis shoot development. *Development*, **122**, 3799–3807.
6. Yasutani,I., Ozawa,S., Nishida,T., Sugiyama,M. and Komamine,A. (1994) Isolation of temperature-sensitive mutants of *Arabidopsis thaliana* that are defective in the redifferentiation of shoots. *Plant Physiol.*, **105**, 815–822.
7. Kim,D., Yang,J., Gu,F., Park,S., Combs,J., Adams,A., Mayes,H.B., Jeon,S.J., Bahk,J.D. and Nielsen,E. (2021) A temperature-sensitive FERONIA mutant allele that alters root hair growth. *Plant Physiol.*, **185**, 405–423.
8. Konishi,M. and Sugiyama,M. (2003) Genetic analysis of adventitious root formation with a novel series of temperature-sensitive mutants of *Arabidopsis thaliana*. *Development*, **130**, 5637–5647.
9. Konishi,M. and Sugiyama,M. (2006) A novel plant-specific family gene, ROOT PRIMORDIUM DEFECTIVE 1, is required for the maintenance of active cell proliferation. *Plant Physiol.*, **140**, 591–602.
10. Kroeger,T.S., Watkins,K.P., Friso,G., van Wijk,K.J. and Barkan,A. (2009) A plant-specific RNA-binding domain revealed through analysis of chloroplast group II intron splicing. *Proc. Natl. Acad. Sci. U.S.A.*, **106**, 4537–4542.
11. Francs-Small,C.C., Kroeger,T., Zmudjak,M., Ostersetzer-Biran,O., Rahimi,N., Small,I. and Barkan,A. (2012) A PORR domain protein required for *rpl2* and *ccmF(C)* intron splicing and for the biogenesis of c-type cytochromes in Arabidopsis mitochondria. *Plant J.*, **69**, 996–1005.
12. Daras,G., Rigas,S., Alatzas,A., Samiotaki,M., Chatzopoulos,D., Tsitsekian,D., Papadaki,V., Templalexis,D., Banilas,G., Athanasiadou,A.M., *et al.* (2019) LEFKOTHEA regulates nuclear and chloroplast mRNA splicing in plants. *Dev. Cell*, **50**, 767–779.
13. Wang,C., Blondel,L., Quadrado,M., Dargel-Graffin,C. and Mireau,H. (2022) Pentatricopeptide repeat protein MTSF3 ensures mitochondrial RNA stability and embryogenesis. *Plant Physiol.*, **2022**, 669–681.
14. Clough,S.J. and Bent,A.F. (1998) Floral dip: a simplified method for Agrobacterium-mediated transformation of *Arabidopsis thaliana*. *Plant J.*, **16**, 735–743.
15. Van Leene,J., Eeckhout,D., Persiau,G., Van De Slijke,E., Geerinck,J., Van Isterdael,G., Witters,E. and De Jaeger,G. (2011) Isolation of transcription factor complexes from Arabidopsis cell suspension cultures by tandem affinity purification. *Methods Mol. Biol.*, **754**, 195–218.
16. Koprivova,A., des Francs-Small,C.C., Calder,G., Mugford,S.T., Tanz,S., Lee,B.R., Zechmann,B., Small,I. and Kopriva,S. (2010) Identification of a pentatricopeptide repeat protein implicated in splicing of intron 1 of mitochondrial *nad7* transcripts. *J. Biol. Chem.*, **285**, 32192–32199.
17. Wang,C., Aube,F., Quadrado,M., Dargel-Graffin,C. and Mireau,H. (2018) Three new pentatricopeptide repeat proteins facilitate the splicing of mitochondrial transcripts and complex I biogenesis in Arabidopsis. *J. Exp. Bot.*, **69**, 5131–5140.
18. Wang,C., Aube,F., Planchard,N., Quadrado,M., Dargel-Graffin,C., Nogue,F. and Mireau,H. (2017) The pentatricopeptide repeat protein MTSF2 stabilizes a *nad1* precursor transcript and defines the 3' end of its 5-half intron. *Nucleic Acids Res.*, **45**, 6119–6134.
19. Sabar,M., Balk,J. and Leaver,C.J. (2005) Histochemical staining and quantification of plant mitochondrial respiratory chain complexes using blue-native polyacrylamide gel electrophoresis. *Plant J.*, **44**, 893–901.
20. Despres,B., Delseny,M. and Devic,M. (2001) Partial complementation of embryo defective mutations: a general strategy to elucidate gene function. *Plant J.*, **27**, 149–159.
21. Wang,C., Fourdin,R., Quadrado,M., Dargel-Graffin,C., Tolleter,D., Macherel,D. and Mireau,H. (2020) Rerouting of ribosomal proteins into splicing in plant organelles. *Proc. Natl. Acad. Sci. U.S.A.*, **117**, 29979–29987.
22. Otsuka,K., Mamiya,A., Konishi,M., Nozaki,M., Kinoshita,A., Tamaki,H., Arita,M., Saito,M., Yamamoto,K. and Hachiya,T. (2021) Temperature-dependent fasciation mutants provide a link between mitochondrial RNA processing and lateral root morphogenesis. *eLife*, **10**, e61611.
23. Sugiyama,M. (2003) Isolation and initial characterization of temperature-sensitive mutants of *Arabidopsis thaliana* that are impaired in root redifferentiation. *Plant Cell Physiol.*, **44**, 588–596.
24. Shen,K., Pender,C.L., Bar-Ziv,R., Zhang,H., Wickham,K., Willey,E., Durieux,J., Ahmad,Q. and Dillin,A. (2022) Mitochondria as cellular and organismal signaling hubs. *Annu. Rev. Cell Dev. Biol.*, **38**, 179–218.
25. Chandel,N.S. (2015) Evolution of mitochondria as signaling organelles. *Cell Metab.*, **22**, 204–206.
26. Van Aken,O. (2021) Mitochondrial redox systems as central hubs in plant metabolism and signaling. *Plant Physiol.*, **186**, 36–52.
27. Mittler,R., Vanderauwera,S., Gollery,M. and Van Breusegem,F. (2004) Reactive oxygen gene network of plants. *Trends Plant Sci.*, **9**, 490–498.
28. Berkowitz,O., De Clercq,I., Van Breusegem,F. and Whelan,J. (2016) Interaction between hormonal and mitochondrial signalling during growth, development and in plant defence responses. *Plant Cell Environ.*, **39**, 1127–1139.
29. Motte,H., Vereecke,D., Geelen,D. and Werbrouck,S. (2014) The molecular path to in vitro shoot regeneration. *Biotechnol. Adv.*, **32**, 107–121.
30. Su,Y.H. and Zhang,X.S. (2014) In: Galliot,B. (ed.) *Current Topics in Developmental Biology*. Academic Press, Vol. **108**, pp. 35–69.
31. Huang,S., Van Aken,O., Schwarzländer,M., Belt,K. and Millar,A.H. (2016) The roles of mitochondrial reactive oxygen species in cellular signaling and stress response in plants. *Plant Physiol.*, **171**, 1551–1559.
32. Mhamdi,A. and Van Breusegem,F. (2018) Reactive oxygen species in plant development. *Development*, **145**, dev164376.
33. Brown,G.G., Colas des Francs-Small,C. and Ostersetzer-Biran,O. (2014) Group II intron splicing factors in plant mitochondria. *Front. Plant Sci.*, **5**, 35.
34. Lambowitz,A.M. and Zimmerly,S. (2011) Group II introns: mobile ribozymes that invade DNA. *Cold Spring Harb. Perspect. Biol.*, **3**, a003616.
35. Bonen,L. (2008) *Cis*- and *trans*-splicing of group II introns in plant mitochondria. *Mitochondrion*, **8**, 26–34.

36. Galej,W.P., Toor,N., Newman,A.J. and Nagai,K. (2018) Molecular mechanism and evolution of nuclear pre-mRNA and group II intron splicing: insights from cryo-electron microscopy structures. *Chem. Rev.*, **118**, 4156–4176.
37. Sultan,L.D., Mileshina,D., Grewe,F., Rolle,K., Abudraham,S., Glodowicz,P., Niazi,A.K., Keren,I., Shevtsov,S., Klipcan,L., *et al.* (2016) The reverse transcriptase/RNA maturase protein MatR is required for the splicing of various group II introns in Brassicaceae mitochondria. *Plant Cell*, **28**, 2805–2829.
38. Edris,R., Sultan,L.D., Best,C., Mizrahi,R., Weinstein,O., Chen,S., Kamennaya,N.A., Keren,N., Zer,H., Zhu,H., *et al.* (2023) Root primordium defective 1 encodes an essential PORR protein required for the splicing of mitochondria encoded group II introns and for respiratory complex I biogenesis. *Plant Cell Physiol.*, https://doi.org/10.1093/pcp/pcad101.
39. Wang,C., Quadrado,M. and Mireau,H. (2023) Interplay of endonucleolytic and exonucleolytic processing in the 3'-end formation of a mitochondrial *nad2* RNA precursor in Arabidopsis. *Nucleic Acids Res.*, **51**, 7619–7630.

Received: August 8, 2023. **Revised:** January 6, 2024. **Editorial Decision:** January 20, 2024. **Accepted:** January 25, 2024